Low-Cost Flight Control System for a Small Autonomous Helicopter

Jonathan M. Roberts[1], Peter I. Corke[1] & Gregg Buskey[2,1]

[1]CSIRO Manufacturing & Infrastructure Technology
PO Box 883, Kenmore, Qld 4069, Australia

[2]University of Queensland
St. Lucia, Qld 4066, Australia

Abstract

In this paper we describe a low-cost flight control system for a small (60 class) helicopter which is part of a larger project to develop an autonomous flying vehicle. Our approach differs from that of others in not using an expensive inertial/GPS sensing system. The primary sensors for vehicle stabilization are a low-cost inertial sensor and a pair of CMOS cameras. We describe the architecture of our flight control system, the inertial and visual sensing subsystems and present some control results.

1 Introduction

We use a small helicopter as an experimental testbed for research into control using visual and inertial sensors. This is a challenging environment due to the simultaneous needs for low weight, low power consumption and high reliability in the presence of extreme vibration. Our helicopter is shown in Figure 1. It is a commercially available 60-size radio-controlled helicopter fitted with a number of custom-made automation system components.

Figure 1: The CMIT Experimental Autonomous Helicopter.

Our approach to control differs to that of many [1–4] in that we do not employ a high performance inertial/GPS sensor. These devices, such as the Novotel RT2 Millennium and the Trimble TANS Quadrex, provide good quality information about the state of the vehicle at 10 Hz which greatly simplifies the control problem.

Our primary sensors are low-cost inertial, magnetic and stereo vision. The first two run at 50 Hz which is sufficient to control the attitude of the helicopter while the latter runs at 10 Hz to facilitate velocity and position control. The stereo vision system provides height relative to the ground (unlike GPS which gives less useful absolute height) and also speed from optical flow between consecutive frames.

Others have pursued the use of these particular sensor modalities to helicopter control, notably Omidi [5] and Srinivasen and Chaal [6]. Omidi's vehicle is significantly larger than ours and the computer technology used was bulkier and heavier than its equivalent today. Srinivasen etal had the state estimation and control algorithms running on a ground-based computer from telemetry data, and the demands were up-linked through a standard radio control (RC) signal.

The remainder of the paper is organised as follows. Section 2 describes the architecture of our helicopter system, while sections 3 and 4 describe our low-cost inertial sensor and recent closed-loop control results. Section 5 describes the vision system for height and speed estimation, while section 6 concludes.

2 System Architecture

2.1 The helicopter

Figure 1 shows the CMIT Experimental Autonomous Helicopter. This helicopter is a commercially available 60 size radio-controlled helicopter fitted with a number of custom-made automation system components.

2.2 Sensors

The helicopter is equipped with the following sensors:

1. downward-looking colour CMOS stereo camera pair,

2. forward facing colour CMOS camera,

3. full 6-dof inertial and magnetic heading platform,

4. human pilot radio commands,

5. rotor RPM counter and

6. battery voltage sensing.

2.3 System design

The overall system design is shown in Figure 2. All processing is performed on-board the helicopter with a low-speed radio modem link to a laptop computer on the ground. This link is only used for tuning control gains and general monitoring. There are two computer systems on-board, the flight computer and control computer.
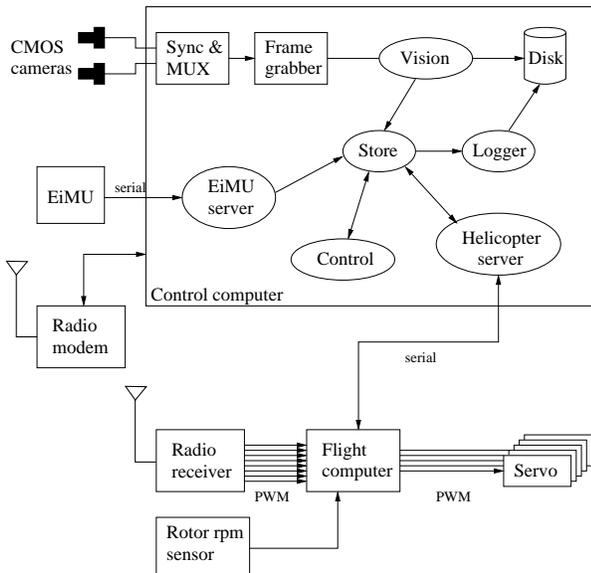

Figure 2: The overall system setup.

The flight computer acts as the interface to the helicopter and is located in the nose. It is based on an in-house developed dual HC12 micro-processor board. The flight computer handles all PWM signals and also handles AtoD, DtoA and digital IO tasks. This brings all the helicopter specific wiring to a central point and hence makes interfacing with the control computer simple. The control computer and flight computer communicate via a standard RS232 serial link.

A key element of the flight computer is an FPGA based safety card that contains five solid-state relays for the five servo channels. This card is designed to allow a human test-pilot to take control quickly and easily in the event of an emergency, or if the computer control of the helicopter is unsatisfactory during development.

The control computer is housed in a carbon-fibre tube mounted underneath the helicopter. As well as providing environmental protection for the computer stack, the carbon-fibre tube also provides very good RF shielding, which is critical for the radio receiver. The control computer is responsible for actually flying the helicopter. It is here that the sensor data is collected, stored and processed. The control computer is based on PC104 and PC104-Plus cards (Figure 3).
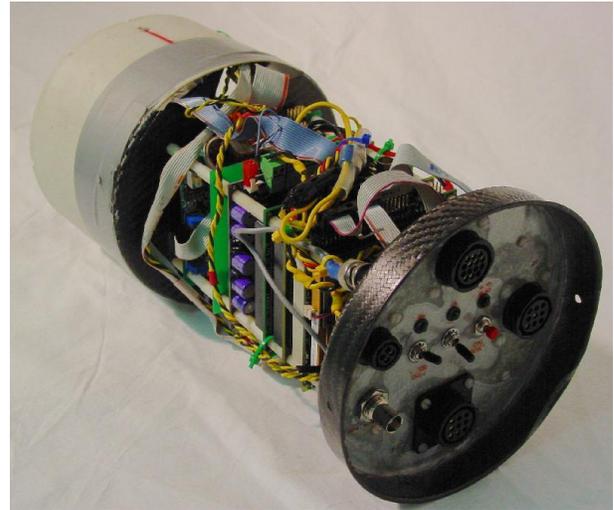

Figure 3: The control computer.

The software system is based on the LynxOS real-time operating system (LynxOS) from Lynuxworks, Inc. At the heart of the software system is the so-called 'store'. This is a generic data broker that is used to exchange data within the system. All sensor data can be logged to the solid-state disk and recovered for off-line analysis.

3 Attitude Estimation

It is essential that the control system can control the attitude of the helicopter. This implies that the attitude of the helicopter must be measured some how. We decided to use an Inertial Measurement Unit (IMU) and compass to perform this task. Other options include vision and multiple GPS receivers. However, these last two options are potentially less robust and more expensive (both in terms of hardware and cost).

3.1 The EiMU

A prime focus of our project is to develop a low-cost flight control system. Commercially available IMUs of the quality required for this application, tend to be expensive (US$5-10k) and heavy (approximately 500-700g). They also tend to be 'black boxes' and contain proprietary filtering algorithms. After much wasted time attempting to use a commercial system in this high-vibration environment, we decided to design and build our our IMU and compass.

Our unit is known as the Embedded inertial Measurement Unit, EiMU, pronounced "emu" like the bird (Figure 4). It is small in size (50mm x 50mm x 50mm) and very lightweight (65g). It consists of a central sensor block machined from magnesium alloy to which the five inertial sensors are precisely mounted. These sensors are three Murata ENC-03J solid-state rate gyros, and two Analog Devices dual-axis ADXL202JQC accelerometers. At the heart of the EiMU is an HC12 based micro-controller board with both serial and Canbus interface. The final element of the EiMU is the magnetometer board. This contains three Honeywell HMC1001/2 magnetometers.

The EiMU is mounted in the control computer tube (underneath the helicopter). It is simply vibration isolated using lightweight springs and foam dampers.
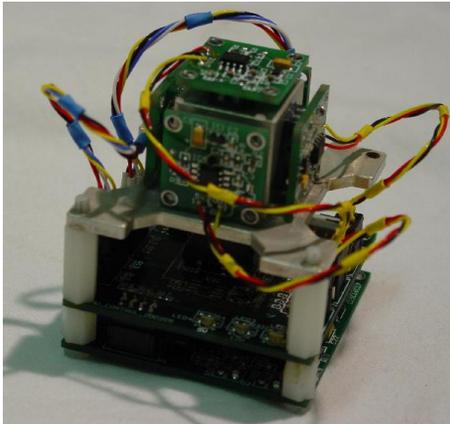

Figure 4: The EiMU.

3.2 Complementary filtering

In order to determine the attitude of the helicopter a complementary filter was implemented for each rotational axis (roll, pitch and heading). The idea of a complementary filter is to use the complementary features of the two inertial sensor types to maximum effect.

Rate gyros measure the rate of rotation about a given axis. The angle of rotation about that axis can therefore be calculated by integrating the angular rate. However, any constant errors in rate measurement will also be integrated and hence the angle measurement will drift. The rate of drift depends on the quality and temperature of the gyros used.

Accelerometers, can be used to directly measure tilt angles (roll and pitch) with respect to gravity. High accuracy tilt measurement using these sensors is possible in a static environment, but impossible in the highly dynamic and high vibration environment of a small helicopter.

The complementary filter is therefore a way of combining the positive features of both of these types of sensors. Figure 5 shows the structure of the complementary filter used. The filter works by calculating an error signal between the estimated angle (θ) and a reference angle (θ_{ref}) calculated directly from the accelerometers. A scaled value of this error signal is then subtracted from the raw angular rate signal before integration. It should be noted that the rate sensors measure in the body-fixed axis, while the accelerometers measure the tilt in the Earth-fixed axis. The Earth-to-body Jacobian (J) and inverse Jacobian (J^{-1}) are used to do the co-ordinate system translations.
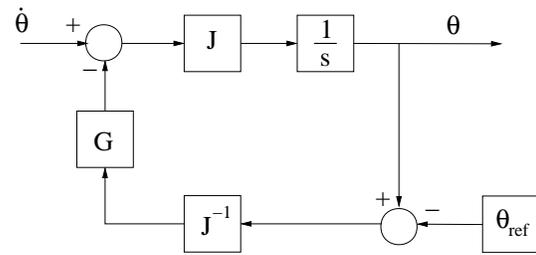

Figure 5: The complementary filter.

The heading reference is determined using the three magnetic components (X, Y and Z) in the horizontal plane. This requires knowledge of the roll and pitch angles. We have chosen to use the estimated roll and pitch angles, from the complementary filter, rather than the reference roll and pitch angles (from the accelerometers) for this calculation.

4 Control

4.1 Rotor speed

The amount of lift generated by the main rotor is determined by the speed of rotation and the pitch (angle of attack) of the rotor blades. In order to achieve fine control of lift and hence height, it is desirable to maintain a fixed rotor speed. Changes in lift are then obtained using the collective only (pitch of the main rotor blades). Changing the

rotor speed significantly using the throttle is undesirable as this process has an inherent and significant delay.

A throttle controller was therefore developed to maintain a fixed rotor speed. The controller was a PI controller with feed forward from the collective demand. A Hall-effect sensor was installed on the tail rotor drive pinion to measure main rotor RPM. The flight computer was used to count pulses and hence measures the main rotor speed.

4.2 Attitude

Attitude control is achieved using three independent proportional controllers on each angular axis (roll, pitch and yaw). Note that roll and pitch are controlled using the two cyclic controls which effectively command roll and pitch rates respectively. Simple proportional control is therefore adequate for the task. Heading control is more complicated however.

The yaw rate of a helicopter is controlled by adjusting the thrust of the tail rotor, which has the job of counteracting the torque of the main rotor while at the same time adding (or subtracting) torque in order to rotate the helicopter. Most small helicopters come equipped with a so-called heading lock system, which is actually a yaw rate controller. Helicopters of this size are almost impossible to fly without these systems. We decided to leave the existing yaw rate controller in place and hence in the control loop for safety reasons. If our system is shutdown for any reason during testing, the backup pilot must take over. Leaving the yaw rate controller on helps with smooth transfers between automatic and manual control. It also allows us to use a simple proportional controller (like the roll and pitch controller).

Figure 6 shows the performance of the three controllers during a typical flight. Note that the pilot still 'flies' the helicopter. His roll, pitch and yaw commands are now interpreted as roll angle, pitch angle and heading angle commands. These are read by the control computer and used as the demands to the three controllers.

5 Vision

We use vision to provide estimates of vehicle height and motion at 10 Hz from images of natural undulating grassy terrain with no artificial landmarks. The significant issues are computational complexity and robust estimation that can handle mismatched features. The algorithms are implemented as tightly written C code and executes in around 80 ms on the helicopter's 800 MHz P3 processor.
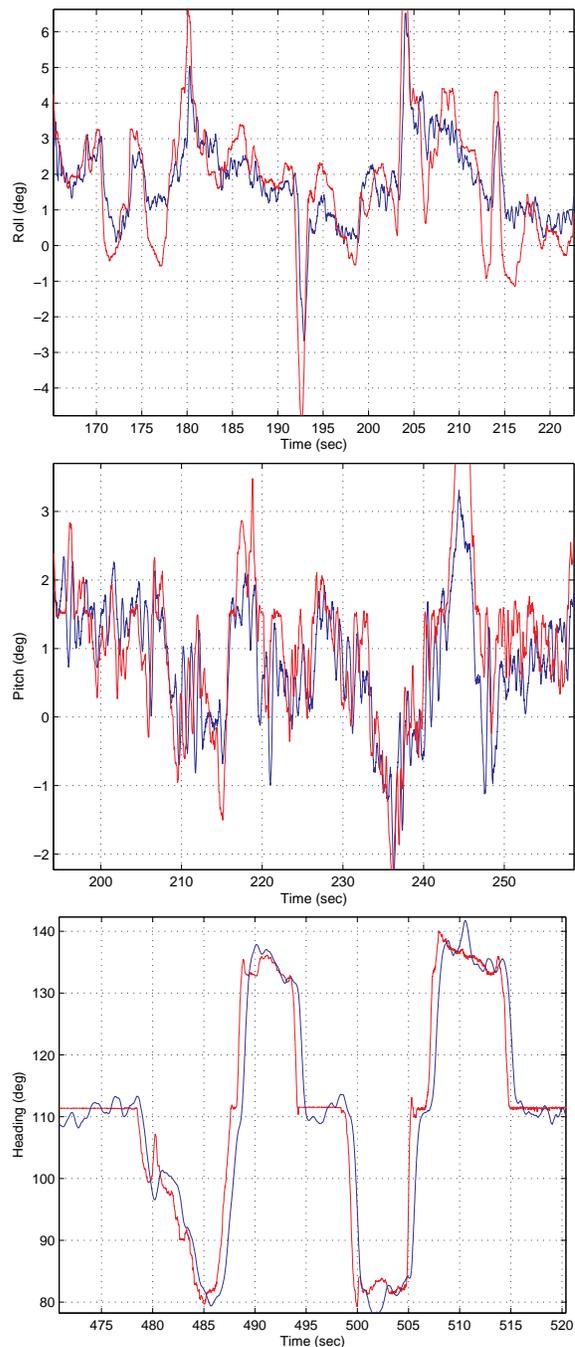

Figure 6: Roll, pitch and heading angle control.

5.1 Height estimation

Estimating height of the vehicle above the ground is required for two purposes: input to the height regulation loop, and to scale estimated optical flow into speed across the ground. A more complete description of our height es-

Figure 7: CMOS camera.

timation system is given in [7]. Notable differences since are the sensors and their placement. The Videre Design ST1 camera head has been replaced with two 1/3 inch in-house color CMOS cameras (Figure 7) mounted directly to the carbon fibre computer housing in order to achieve a more rigid mount and a longer baseline (305 mm). We process individual fields and after de-interlacing have a pair of images 144×384 at 50 Hz although we normally skip fields and process at 10 Hz.

The approach [7] is based on estimating correspondence of corner features [8–10] between the left and right image. We use approximate epipolar constraints to minimise the search space and possible conjugate points are verified by cross correlation. The resulting disparities have a number of outliers due to incorrect matching so a clustering technique is used to find the largest consistent set of disparities. Results logged from the helicopter are shown in Figure 8 with disparity converted to height. The standard deviation is that within the cluster, the lower plot shows the number of matched features (blue) and the number of features within the cluster (green).

5.2 Motion estimation

Tracking corner features between consecutive frames provides the raw information for velocity estimation and odometry. Since the corners are already computed for the stereo process we do not have to recompute them for motion estimation. The two subproblems are correspondence and motion estimation, which are not independent. Currently we use a simple strategy for establishing correspondence which assumes that the matching points lies within a disk of fixed radius from a point predicted based on image velocity from the previous frame (we are currently implementing this prediction based on information obtained from the inertial sensor). Theoretically knowledge of the correspondence can be used to estimate the full 6DOF velocity screw, for example by estimating [11] and decomposing [11,12] the fundamental matrix. In practice we find this method to be not robust with respect to
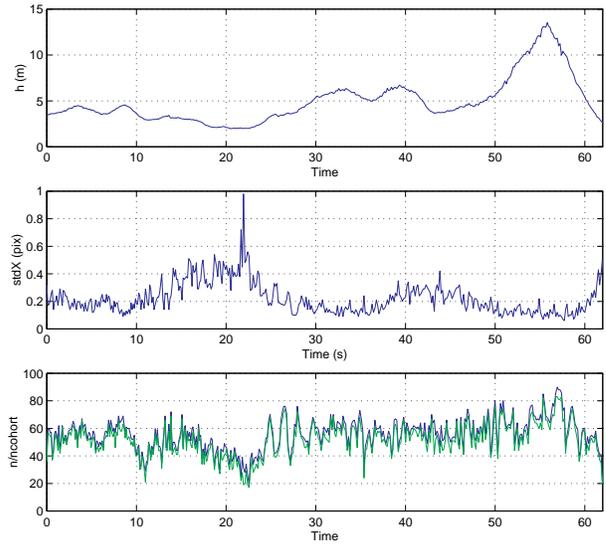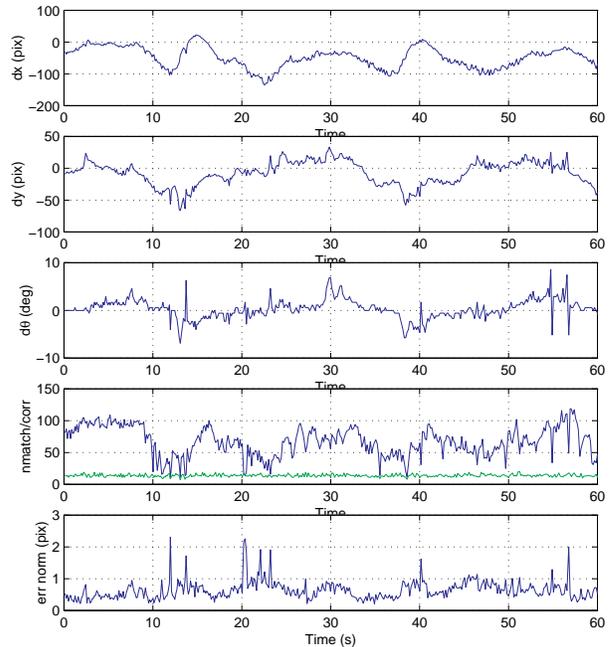

Figure 8: Online height results.

Figure 9: Online image motion results.

errors introduced by relative camera motion and the non-simultaneous pixel sampling characteristics of the CMOS sensors. Figure 9 shows x-direction (forward) motion results for high speed (piloted) flight where the velocity exceeds 100pix/frame.

Figure 10 shows how the visual information is combined with inertial data in a complementary filter. The top graph shows the x-direction acceleration (blue) with the estimated gravity component (green) obtained from roll and
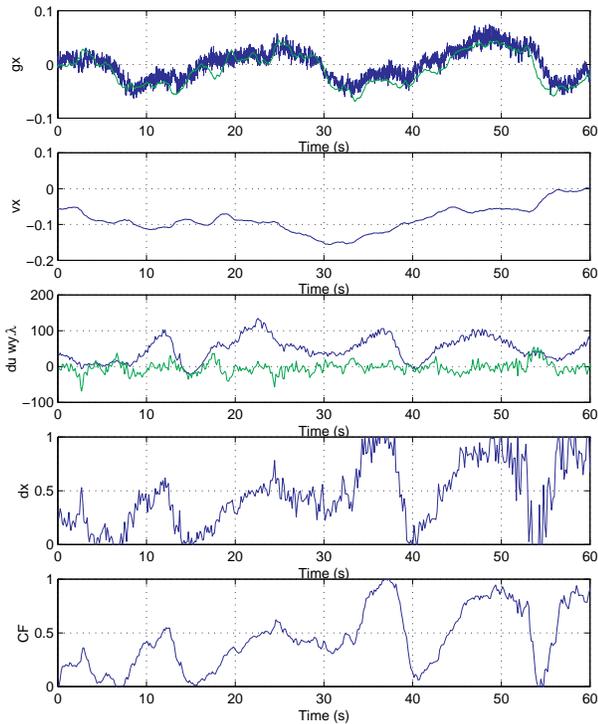
Figure 10: Online ground speed results.

pitch information. The difference is due to motion of the vehicle and when integrated gives the signal shown in the second graph. The third graph shows the x-direction visual velocity as estimated above (blue) and the component due to pitch rate (green) in pixels/frame. After multiplying by height (obtained from stereo disparity) we obtain the visual estimate of ground speed, fourth graph. The bottom graph shows the output of the complementary filter which combines acceleration and visual velocity into ground speed in m/s. The zero velocity points correspond to turns as confirmed by the high values of $d\theta$ in Figure 9.

6 Conclusion

This paper has presented a brief overview of a low-cost flight control system for a small helicopter and presented experimental results. The components of the flight-control system include a 6-axis inertial sensor, magnetometer and stereo vision system for height and motion estimation, and an attitude control system. The work presented is part of an ongoing research project and we hope in the near future to demonstrate stable hover over a point target. The approach used differs from that of others in not using a high-performance inertial/GPS sensor for control, and having all computation and sensor processing onboard.

Work is also underway to more closely integrate the visual and inertial sensors to overcome their complementary deficiencies and to reduce the computational requirement for visual motion estimation, and also to investigate learning based control schemes.

Acknowledgements

References

[1] A. Conway, *Autonomous control of an Unstable Model helicopter Using Carrier Phase GPS Only*. PhD thesis, Dept Electrical Engineering, Stanford University, Stanford, CA 94305, March 1995.

[2] T. Koo, H. Shim, and O. Shakernia, "Hierarchical hybrid system design on berkely uav," in *International Aerial Robotics Competition*, 1998.

[3] K. Harbick, J. Montgomery, and G. Sukhatme, "Planar spline trajectory following for an autonomous helicopter," in *IEEE International Symposium on Computational Intelligence in Robotics and Automation*, (Banff Canada), 2001.

[4] R. Miller, O. Amidi, and M. Delouis, "Arctic test flights of the cmu autonomous helicopter," in *Association for Unmanned Vehicle Systems International 1999. 26th Anuual Symposium.*, vol. Received before publications, yet to get details., (Baltimore, MD), 1999.

[5] O. Amidi, *An Autonomous Vision-Guided Helicopter*. PhD thesis, Dept of Electrical and Computer Engineering, Carnegie Mellon University, Pittsburgh, PA 15213, 1996.

[6] "Biorobotic vision laboratory." http://cvs.anu.edu.au/bioroboticvision/brv.html, 2002.

[7] P. Corke, P. Sikka, and J. Roberts, "Height estimation for an autonomous helicopter," in *International Symposium on Experimental Robotics*, 2000.

[8] R. Deriche and G. Giraudon, "A computational approach for corner and vertex detection," *Int. J. Computer Vision*, vol. 10, no. 2, pp. 101–124, 1993.

[9] D. Charnley, C. G. Harris, M. Pike, E. Sparks, and M. Stephens, "The DROID 3D Vision System - algorithms for geometric integration," Tech. Rep. 72/88/N488U, Plessey Research Roke Manor, December 1988.

[10] J. M. Roberts, *Attentive Visual Tracking and Trajectory Estimation for Dynamic Scene Segmentation*. PhD thesis, University of Southampton, UK, dec 1994.

[11] R. Hartley and A. Zisserman, *Multiple View Geometry in computer vision*, ch. 8-10, pp. 219–293. Cambridge University Press, 2001.

[12] O. Faugeras, *Three-Dimensional Computer Vision: A Geometric Viewpoint*, ch. 7, pp. 245–296. MIT Press, 1993.